Catalysis Science & Technology

Accepted Manuscript

ROYAL SOCIETY OF CHEMISTRY

www.rsc.org/catalysis

RSCPublishing

ARTICLE

Ag-Pd alloy supported on amine-functionalized UiO-66 as an efficient synergetic catalyst for dehydrogenation of formic acid at room temperature

Shu-Tao Gao, Weihua Liu, Cheng Feng*, Ning-Zhao Shang, Chun Wang*

College of Science, Agricultural University of Hebei, Baoding 071001, China

Cite this: DOI: 10.1039/x0xx00000x

Received 00th January 2015,
Accepted 00th January 2015

DOI: 10.1039/x0xx00000x

www.rsc.org/

Highly dispersed Ag-Pd alloy deposited on amine-functionalized UiO-66(NH_2-UiO-66) have been successfully prepared with a pre coordination method. The as-synthesized AgPd@NH_2-UiO-66 catalyst exhibited 100% H_2 selectivity and high catalytic activity (TOF = 103 h^{-1}) toward the dehydrogenation of formic acid at room temperature without any additives, which is among the highest values ever reported. Our study further reveals that the synergetic effect between the Ag-Pd alloy and NH_2-UiO-66 support play a key role for the efficient catalytic dehydrogenation of formic acid.

Introduction

Hydrogen (H_2) has been considered as one of the ultimate energy vectors to satisfy the increasing demand for a sustainable and clean energy supply.[1-3] However, controllable storage and release of H_2 remains one of the most difficult challenges on the way to a hydrogen-powered society.[4] Recently, various hydrogen storage chemicals such as sodium borohydride ($NaBH_4$), formic acid (FA, HCOOH) and ammonia borane (NH_3BH_3) derivatives, have been considered to replace classic pressurization or cryogenic liquefaction technology.[5-7] Among them, formic acid (FA, HCOOH), a major byproduct of biomass processing, has been considered as a promising H_2 storage material due to the properties of high energy density, non-toxicity, excellent stability, and with the potential to be regenerated by hydrogenation of carbon dioxide (CO_2).[8-23] Hydrogen stored in FA can be released via a catalytic dehydrogenation reaction (Eq. 1). However, the undesirable dehydration pathway (Eq. 2), which is typically promoted by heating or acidity, should be strictly controlled, as CO impurities are not well tolerated by fuel cells.[24]

$$HCOOH\ (l) \longrightarrow CO_2\ (g) + H_2\ (g) \quad \triangle G_{298} = -48.8 kJ \cdot mol^{-1} \quad (1)$$

$$HCOOH\ (l) \longrightarrow CO\ (g) + H_2\ (g) \quad \triangle G_{298} = -28.5 kJ \cdot mol^{-1} \quad (2)$$

Recently, there have been reports of highly efficient dehydrogenation of FA over homogeneous catalysts at ambient temperatures.[25-27] However, the separation and recycling issues associated with homogeneous catalysts impede their use in practical applications. To address these problems, the design and fabrication of efficient heterogeneous catalysts has received much attention in recent years.[13, 28] In which, bimetallic nanoparticles (NPs) were found to be more active than their single component counterparts for the dehydrogenation of FA.[29] The addition of a second metal is an important approach for tailoring the electronic and geometric structures of NPs to enhance their catalytic activity and selectivity.[30] For example, Ag-Pd alloy[29] and monodisperse Ag-Pd alloy NPs supported on carbon based materials,[8] have been developed for the catalytic dehydrogenation of formic acid. Despite recent progress, the development of efficient and selective heterogeneous catalysts for the hydrogenation of formic acid under mild conditions is still highly desired for practical use. The reports about dehydrogenation of FA at room temperature, especially in the absence of extra additives, are still very few.[1, 17, 23, 31-33] It is well known that the addition of extra additives may lead to severe difficulties in device fabrication.

It has been demonstrated that the synergetic interaction between metal and support, the type of the support, and the dispersity of the metal nanoparticles play an important role for the catalytic performance of the nanocatalysts and the kinetic properties of FA dehydrogenation.[34] Currently, the incorporation of metal nanoparticles in metal-organic frameworks (MOFs) has received much attention in catalysis

since MOFs have large internal surface areas, uniform but tunable cavities, and are suited to stabilize certain classes of metal nanoparticles.[35] Most recently, Dai et al. have successfully immobilized Ag-Pd NPs on the metal-organic frameworks (MIL-101 or ZIF-8) by using a simple liquid impregnation method, and all of them have been found to be active for the decomposition of FA at 80 °C in the presence of sodium formate.[36, 37] Regrettably, all of them need extra additives and elevated temperature which are harmful to the practical application of FA as H_2 storage material. Moreover, the stability of the catalysts need improved and the aggregation of the metal nanoparticles was observed, which would decrease the catalytic activity and reusability of the catalyst.

NH_2-UiO-66 is a zirconium (IV)-based MOF, which has received significant attention in recent years due to its unique properties such as light harvesting, high thermal and chemical stability, tunable pore sizes, high specific surface areas and the possibility to functionalize.[38-44]

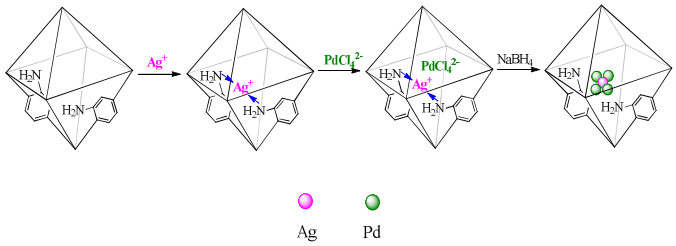

Scheme 1 Schematic representation of the synthesis process of the AgPd@NH_2-UiO-66

Herein, we report a facile strategy to fabricate well dispersed Ag-Pd alloy NPs encapsulated in the pores of amine-functionalized UiO-66 (NH_2-UiO-66) via a pre coordination method. The Ag^+ and $PdCl_4^{2-}$ were immobilized into the pores of NH_2-UiO-66 through the coordination or electrostatic interaction with the amino groups in the MOF. After reduction with sodium borohydride, the Ag-Pd alloy was anchored into the pores of NH_2-UiO-66. The amino groups in the MOF play a crucial role in the nucleation and growth of Ag-Pd alloy. The synthesis process of the AgPd@NH_2-UiO-66 is schematically shown in Scheme 1. The as-synthesized AgPd@NH_2-UiO-66 catalyst exhibited high catalytic activity and 100% H_2 selectivity for the dehydrogenation of formic acid at room temperature without any additives. To the best of our knowledge, this is the first report about MOFs supported Ag-Pd alloy NPs for catalytic dehydrogenation of formic acid at room temperature in the absence of extra additives.

Experimental

Chemicals

Zirconium chloride ($ZrCl_4$), palladium (II) chloride ($PdCl_2$, AR), sodium borohydride ($NaBH_4$, 96%) and 2-NH_2-terephthalic acid were obtained from Aladdin Reagent Limited Company. *N*, *N*-Dimethylformamide (DMF) and hydrochloric acid (HCl, 37%) were obtained from Chengxin Chemical Reagents Company (Baoding, China). Silver nitrate ($AgNO_3$, AR) and formic acid (HCOOH, 98%) were purchased from Huaxin Co., Ltd. (Baoding, China). All materials were used as received without further purification.

Characterizations

The size and morphology of the nanoparticles were observed by transmission electron microscopy (TEM) using a JEOL model JEM-2011(HR) at 200 kV. The X-ray diffraction (XRD) patterns of the samples were recorded with a Rigaku D/max 2500 X-ray diffractometer using Cu *Kα* radiation (40 kV, 150 mA) in the range 2θ = 5° - 80°. X-ray photoelectron spectroscopy (XPS) was performed with a PHI 1600 spectroscope using Mg *Kα* X-ray source for excitation. The surface area, total pore volume and pore size distribution of the samples were measured at 77 K by nitrogen adsorption using a V-Sorb 2800P volumetric adsorption equipment (Jinaipu, China). The metal content of the materials was analyzed by a T.J.A. ICP-9000 type inductively coupled plasma atomic emission spectroscopy (ICP-AES) instrument. Detailed analyses for CO_2, H_2 and CO were performed on SP-2000 (Beijing Beifen Ruili Analytical Instrument CO., Ltd.). The H_2 and CO_2 compositions were measured by GC spectrum using TCD, while CO was measured by GC spectrum using FID-Methanator.

Synthesis of NH_2-UiO-66

NH_2-UiO-66 was synthesized according to the reported process in the literature.[36] In a typical synthesis, $ZrCl_4$ (0.2332 g, 1.0 mmol) and 2-NH_2-benzenedicarboxylate (0.1812 g, 1.0 mmol) were dissolved in DMF (50 mL), and then the solution was transferred to a 100 mL Tefon-lined stainless steel autoclave. The autoclave was sealed and heated in an oven at 120 °C for 48 h under autogenous pressure, after cooled naturally, the sample was purified with anhydrous methanol for several times to make sure that the occluded DMF molecules were eliminated, the yellow NH_2-UiO-66 product was dried in a vacuum at 80 °C for 12 h.

Synthesis of AgPd@NH_2-UiO-66

Typically, for the preparation of Ag_1Pd_4@NH_2-UiO-66, 100 mg NH_2-UiO-66 was dispersed in 6.8 mL of 5.8 mmol L^{-1} silver nitrate (0.04 mmol) solution and stirred at room temperature for 1 h. Then, 28 mL of 5.7 mmol L^{-1} H_2PdCl_4 solution (0.16 mmol) was added and the obtained solution was stirred at room temperature for 4 h. The resulting mixture was then reduced by 2 mL $NaBH_4$ (1 mol L^{-1}) solution with vigorous stirring to yield Ag_1Pd_4@NH_2-UiO-66. The preparations of Ag_1Pd_2@NH_2-UiO-66, Ag_1Pd_1@NH_2-UiO-66, Ag_2Pd_1@NH_2-UiO-66, Ag_4Pd_1@NH_2-UiO-66, Ag@NH_2-UiO-66 and Pd@NH_2-UiO-66 catalysts were synthesized with the

above procedure except that the molar ratios of Ag and Pd were 1:2, 1:1, 2:1, 4:1 1:0 and 0:1, respectively. The contents of Ag and Pd in the composite were determined by ICP-AES as shown in Table 1.

To elucidate the presence of synergetic effect of AgPd alloy, Ag_1Pd_4@NH_2-UiO-66 nanoparticles were prepared by step-by-step reduction. In the first step, $AgNO_3$ was adsorbed by NH_2-UiO-66 and reduced by $NaBH_4$ to obtain Ag@NH_2-UiO-66. In the second step, H_2PdCl_4 was further reduced to obtain Ag-Pd bimetallic particles on NH_2-UiO-66.

Table 1 ICP-AES results of AgPd@NH_2-UiO-66 catalysts

Catalysts	Ag (wt%)	Pd (wt%)	Ag-Pd initial composition	Ag-Pd final composition
Ag_1Pd_4@NH_2-UiO-66	3.80	12.59	1:4	1:3.31
Ag_1Pd_2@NH_2-UiO-66	5.51	10.81	1:2	1:1.96
Ag_1Pd_1@NH_2-UiO-66	8.20	7.96	1:1	1.03:1
Ag_2Pd_1@NH_2-UiO-66	10.54	5.46	2:1	1.93:1
Ag_4Pd_1@NH_2-UiO-66	13.10	3.40	4:1	3.80:1

H_2 generation from FA over AgPd@NH_2-UiO-66

The hydrogen production from FA solution was carried out in a 10 mL round-bottomed flask, which was placed in an oil bath with magnetic stirrer at a preset temperature (25 °C, 50 °C and 80 °C). A gas burette filled with water was connected to the reaction flask to measure the volume of released gas. Firstly, 10 mg catalyst and 2 mL distilled water were placed in the round-bottomed flask. Then, the reaction started when 1.0 mL of 1.25 mmol mL^{-1} formic acid was injected into the mixture using a syringe. The volume of the evolved gas was monitored by recording the displacement of water in the gas burette.

The hydrogen gas volume as production per mole of Ag-Pd catalyst per hour was calculated using equation S1 and S2 (see supporting information, †).

Recyclability test

For the recycle stability test, after the dehydrogenation of FA was completed, the catalyst was isolated from reaction solution by centrifugation and washed with water, then dried in a vacuum at 80 °C for 6 h. The dried catalyst was used again in the catalytic dehydrogenation of aqueous FA solution.

Results and discussion

In the preparation process of the AgPd@NH_2-UiO-66, NH_2-UiO-66 was dispersed in $AgNO_3$ solution and stirred at room temperature to confirm that Ag^+ could coordinate with the –NH_2 groups which protrude in the micropores of NH_2-UiO-66. And then, the aqueous solution of H_2PdCl_4 was poured into the mixture and stirred at room temperature, $PdCl_4^{2-}$ could introduced into the framework of NH_2-UiO-66 via electrostatic attraction with Ag^+. And then AgPd nanoparticles were formed in the pores of NH_2-UiO-66 by the reduction of Ag^+ and Pd^{2+} with $NaBH_4$. The method could improve the dispersion and stabilization of metal nanoparticles and prevent metal nanoparticles from escaping or agglomerating. The well dispersed metal nanoparticles are beneficial for the enhancement of catalytic activity of the catalyst.

Characterization of AgPd@NH_2-UiO-66

The crystallographic structure of the as-prepared AgPd@NH_2-UiO-66 sample was examined by powder X-ray diffraction (PXRD). Fig. 1 showed the XRD patterns of (a) NH_2-UiO-66, (b) Pd@ NH_2-UiO-66, (d) Ag_1Pd_4@ NH_2-UiO-66, (e) Ag@NH_2-UiO-66 and (c) Ag_1Pd_4@NH_2-UiO-66 via two step reduction. It can be seen that all the as-prepared samples possess similar XRD patterns at 2θ = 5-10 degree. Compared with NH_2-UiO-66, the characteristic peaks of Ag_1Pd_4@NH_2-UiO-66 at low-angle were diminished, which can be ascribed to that the amount of Pd and/or Ag in the Ag_1Pd_4@NH_2-UiO-66 is relatively high (as determined by ICP, Table 1). To further confirm the integrity of NH_2-UiO-66, we reduced the amount of Pd and/or Ag in the synthesized nanocomposites to 5 wt%, whose PXRD patterns were shown in Fig. S1(†). From which we can observe that there is no apparent loss of crystallinity of NH_2-UiO-66 in Pd@NH_2-UiO-66, Ag@NH_2-UiO-66 and Ag_1Pd_4@NH_2-UiO-66. Furthermore, the wide-angle PXRD pattern of Ag_1Pd_4@NH_2-UiO-66 exhibited a smaller and broader peak between the characteristic peaks of Ag(111) (2θ = 38.03°) and Pd(111) (2θ = 40.1°), indicating the formation of the Ag–Pd alloy, and also suggesting that the well dispersion of Ag-Pd alloy NPs. For Ag_1Pd_4@NH_2-UiO-66 prepared via step-by-step reduction, the peak of Ag-Pd bimetallic particle (Fig. 1c) appears at about 38.81°, which was smaller than that of Ag–Pd alloy (39.18°, Fig. 1d).

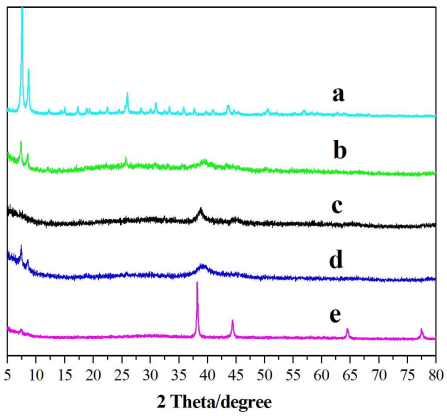

Figure 1 Powder X-ray diffraction patterns for (a) NH_2-UiO-66, (b) Pd@NH_2-UiO-66, (c) Ag_1Pd_4@NH_2-UiO-66 via two step reduction, (d) Ag_1Pd_4@NH_2-UiO-66 and (e) Ag@NH_2-UiO-66

Fig. 2 shows a transmission electron microscopy (TEM) image of the Ag_1Pd_4@NH_2-UiO-66 nanocomposites. The AgPd NPs are homogenously dispersed over the NH_2-UiO-66 with a

narrow particle size distribution of about 3-6 nm. We can see from Fig. 2a that most of the AgPd NPs were encapsulated within the pores of NH_2-UiO-66 with vague distorted lattice fringes, which is mainly due to the charging of the sample under the electron beam especially for the small particles. [45] Moreover, it can be observed that some of the larger AgPd NPs disperse on the surface of the NH_2-UiO-66 have clear lattice fringes. Fig. 2b shows the high-resolution TEM (HRTEM) image of the as-prepared catalyst, wherein the lattice spacing is 0.23 nm, which is between the (111) lattice spacing of face-centered cubic (fcc) Ag (0.24 nm) and fcc Pd (0.22 nm), further suggesting that Ag-Pd is formed as an alloy structure. Fig. S2 and S3 (†) showed the high-angle annular darked scanning TEM (HAADF-STEM) of the Ag_1Pd_4@NH_2-UiO-66 and the related element mapping of C, N, Zr, O, Pd, and Ag, respectively. It can be seen that the element of N, Ag and Pd have a similar distribution map. The results confirmed the hypothesis that we proposed as above about the formation process of the as-prepared catalyst. The line scan and corresponding EDS results unambiguously demonstrated that Ag-Pd was formed as an alloy structure (Fig. S4, †).

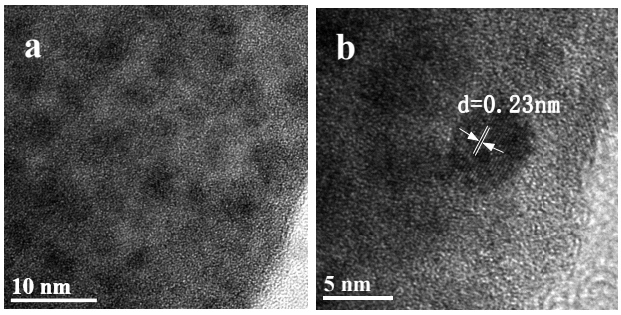

Figure 2 TEM images for the Ag_1Pd_4@NH_2-UiO-66 (a and b)

The N_2 adsorption–desorption isotherms of NH_2-UiO-66 and Ag_1Pd_4@NH_2-UiO-66 are shown in Fig. 3. The BET surface areas of NH_2-UiO-66 and Ag_1Pd_4@NH_2-UiO-66 were 955.7 and 406.4 m^2 g^{-1}, respectively. The large decrease in the amount of N_2 adsorption and the pore volume (Fig. 3) of Ag_1Pd_4@NH_2-UiO-66 indicates that the pores of NH_2-UiO-66 were either occupied or blocked by the well dispersed Ag-Pd NPs.

XPS analysis further confirms the presence of Ag, Pd, Zr, C, O and N in the Ag_1Pd_4@NH_2-UiO-66 hybrid composites (Fig. S5, †). As shown in Fig. S5b and S5c, the $3d^{5/2}$ and $3d^{3/2}$ peak of Pd^0 appear at 335.9 eV and 341.2 eV,[32] the $3d^{5/2}$ and $3d^{3/2}$ peak of Ag^0 appear at 367.9 eV and 373.8 eV.[37] The two other peaks in the Fig. S5c are ascribed to the Zr $3p^{1/2}$ and Zr $3p^{3/2}$, respectively. The results are consistent with the values reported in the literature.[36] No obvious peaks of Ag^+ and Pd^{2+} observed, indicating the co-existence of both metals.[36] The curves of Zr 3d region could be deconvoluted into two peaks for Zr $3d^{5/2}$ and Zr $3d^{3/2}$ locating at around 182.53 eV and 184.88 eV, respectively, which in accordance with the initial NH_2-UiO-66.[39] The N1s XPS spectrum of Ag_1Pd_4@NH_2-UiO-66 locates at 400.03 eV, no significant difference has been observed compared with that of NH_2-UiO-66,[39] suggesting that the $-NH_2$ groups can be retained after the reduction processing and they do not coordinate with Ag or Pd metal ions.

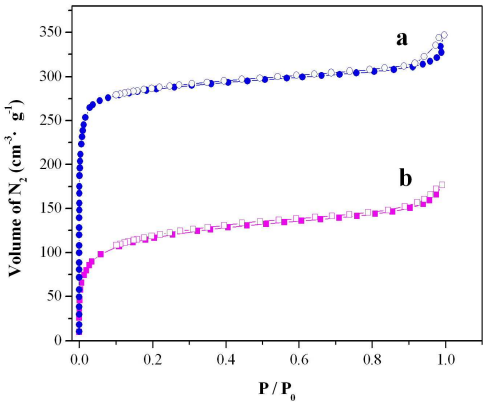

Figure 3 N_2 adsorption-desorption isotherms of (a) NH_2-UiO-66 and (b) Ag_1Pd_4@NH_2-UiO-66 at 77 K. Filled and open symbols represent adsorption and desorption branches, respectively.

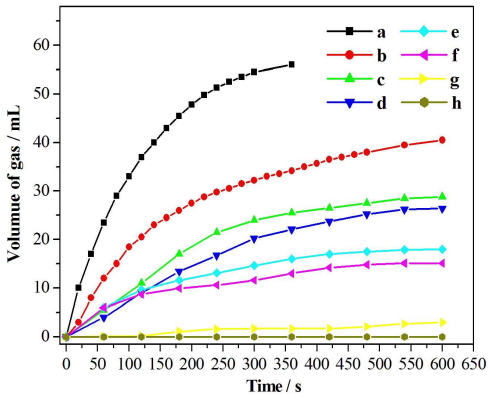

Figure 4 Gas generation by decomposition of FA with different ratios of Ag/Pd supported on NH_2-UiO-66 versus time at 80 °C (n_{FA} = 1.25 mmol, n_{metal} : n_{FA} = 0.01 : 1). (a) Ag_1Pd_4@NH_2-UiO-66, (b) Ag_1Pd_4@NH_2-UiO-66 via step-by-step reduction. (c) Pd@NH_2-UiO-66, (d) Ag_1Pd_2@NH_2-UiO-66, (e) Ag_1Pd_1 @NH_2-UiO-66, (f) Ag_2Pd_1@NH_2-UiO-66, (g) Ag_4Pd_1@NH_2-UiO-66, (h) Ag@NH_2-UiO-66.

Fig. 4 shows the plots of the gas (CO_2 + H_2) generated versus reaction time during the dehydrogenation of FA over different catalysts that with different ratios of Ag/Pd at 80 °C. Catalytic performances of all the catalysts were studied based on the amount of gases measured volumetrically during the reaction. Their catalytic activities were strongly depended on the composition of Ag-Pd clusters.[37] Remarkably, the Ag_1Pd_4@NH_2-UiO-66 hybrid shows the highest activity among all the catalysts prepared in this work. It is almost full conversion of FA to H_2 within 5 min (x_a=97.3%, eqn S1†). The initial turnover frequency (TOF, eqn S2†) over Ag_1Pd_4@NH_2-UiO-66 was measured to be 893 h^{-1} at 80 °C. The exclusive formation of H_2 and CO_2 without CO formation has been confirmed by gas chromatography (GC) analyses (Fig. S6 and

S7, †), indicating the excellent H_2 selectivity for formic acid dehydrogenation catalyzed by Ag_1Pd_4@NH_2-UiO-66. Almost no reactivity was observed for Ag@NH_2-UiO-66, and less than 25 mL gas was generated over 10min for Pd@NH_2-UiO-66, indicating that AgPd alloy provides a necessary synergistic effect on catalysis and Ag_1Pd_4@NH_2-UiO-66 is the optimum catalyst for catalyzing the dehydrogenation of FA.

In addition, we evaluated the catalytic activity of Ag_1Pd_4@NH_2-UiO-66 via step-by-step reduction. The H_2 generation rates and amount of total from FA were significantly lower than that of Ag_1Pd_4@NH_2-UiO-66 (Fig. 4b). The results again confirm that the AgPd alloy in Ag_1Pd_4@NH_2-UiO-66 play a pivotal role in accelerating FA dehydrogenation.

To our delight, even at 25 °C, the TOF value at 45% conversion of FA to H_2 within 20 min is as high as 103 h^{-1} (Fig. 5), which is higher than most of the reported heterogeneous catalysts for this reaction without extra additives at room temperature, and is even comparable to most of those with additives or/and taking place at elevated temperatures (Table 2). The TOF at different temperatures as shown in Table 2 were calculated from the slope of the linear part of each plot from Fig. 5. The Arrhenius plot of ln TOF versus 1/T for the catalyst was plotted in Fig. 5, from which the obtained apparent activation energy (*E*a) of the reaction was approximately 29.66 kJ/mol, being lower than most of the reported values.

Compared with the results reported in the literature,[36, 37] the application of NH_2-UiO-66 as support can enhance the catalytic activity of AgPd alloy for H_2 generation from FA at room temperature. It is supposed that not only the well dispersion and ultrafine sizes of AgPd alloy on NH_2-UiO-66 but also the properties of weakly basic amino groups were important factors in attaining high catalytic activity.[16] The weakly basic amino group can facilitate the cleavage of O–H bond in FA, which is associated with the rate-determining C–H bond cleavage from the HCOO* intermediate to release H_2.[31]

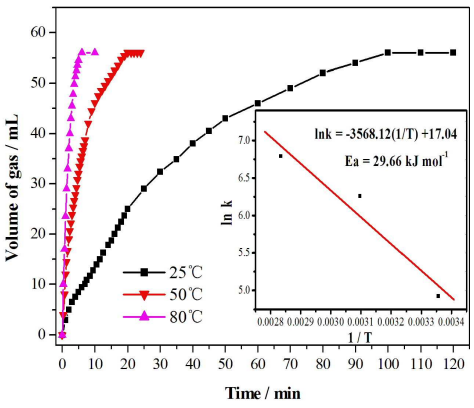

Figure 5 Volume of the generated gas (CO_2 + H_2) versus time, Arrhenius plot (ln(TOF) vs. 1/T).

In addition, the stability of the Ag_1Pd_4@NH_2-UiO-66 catalyst was examined by dehydrogenation of FA at 80 °C (Fig. S8, †). After the complete dehydrogenation of FA, the catalyst was isolated from reaction solution by centrifugation and washed with excess water, then dried in a vacuum at 80 °C. The dried catalyst was used again in the catalytic dehydrogenation of aqueous FA solution. As shown in Fig. S8 (†), the as-synthesized catalysts still exhibit certain catalytic activity without significant loss in activity and selectivity even after the fifth run. The results reliably indicate that the present catalyst possesses high durability and stability during FA decomposition.

Table 2 Catalytic activity of different catalysts for the decomposition of formic acid

Catalyst	Additive (mmol)	Tem. (°C)	TOF (h^{-1})	Ref.
Without additive				
Ag_1Pd_4@NH_2-UiO-66	None	25	103 [a]	This work
Ag_1Pd_4@NH_2-UiO-66	None	50	525 [b]	
Ag_1Pd_4@NH_2-UiO-66	None	80	893 [b]	
AuPd–MnOx /ZIF-8–rGO	None	25	382.1[c]	33
CoAuPd/DNA-rGO	None	25	85.0 [a]	23
AuPd-CeO_2/N-rGO	None	25	52.9 [a]	31
CoAuPd/C	None	25	36.9 [a]	17
$Ag_{0.42}Pd_{0.58}$	None	50	548.8 [a]	29
$Au_{0.41}Pd_{0.59}$	None	50	108.1 [a]	15
Pd- poly(allyl-amine)	None	22	46.1 [a]	32
Ag@Pd core-shell	None	20	15.5 [a]	1
With additive				
$(Co_6)Ag_{0.1}Pd_{0.9}$/RGO	HCOONa	25	453 [a]	28
Pd/MSC-30	HCOONa	25	750 [a]	34
Au/ZrO_2	NEt_3	25	252 [a]	4
AgPd@ZIF-8	HCOONa	80	580 [a]	37
AgPd@MIL-101	HCOONa	80	848 [a]	36
PdAu/ED-MIL-101	HCOONa	90	245.9 [a]	11
PdAu/C-CeO_2	HCOONa	92	141.4 [a]	8
PdAg/C-CeO_2	HCOONa	92	68.5 [a]	8
PdAu@Au/C	HCOONa	92	48.4 [a]	9

a: The TOF value is measured during the first 20 min of the reaction. b: The TOF value is measured during the first 5 min of the reaction. c: The TOF value is measured during the first 10 min of the reaction.

Conclusions

In summary, we have developed a facile strategy to prepare a well dispersed Ag-Pd alloy NPs growing on amine-functionalized NH_2-UiO-66. The as-synthesized catalyst exhibits excellent activity and selectivity for H_2 generation from FA without any additives at 25 ^oC. Our study further reveals that the synergetic effect of Ag-Pd alloy in MOFs for the catalytic dehydrogenation of formic acid.[36, 37] This remarkable improvement of the catalytic performance of the Ag_1Pd_4@NH_2-UiO-66 hybrid may strongly encourage the practical application of FA as a hydrogen storage material in fuel cell applications.

Acknowledgements

This work was financially supported by the National Natural Science Foundation of China (no. 31171698, 31471643), the Innovation Research Program of Department of Education of Hebei for Hebei Provincial Universities (LJRC009), Natural Science Foundation of Hebei Province (B2015204003) and the Natural Science Foundation of Agricultural University of Hebei (LG201404, ZD201506).

Notes and references

College of Science
Agricultural University of Hebei
Baoding 071001, Hebei Province, P. R. China
Fax: (+86)312-7528292
E-mail: chunwang69@126.com (C. Wang); fengchengcctv@163.com (C. Feng)

Electronic Supplementary Information (ESI) available: EDX spectrum, XPS patterns, and elemental mapping of Ag_1Pd_4@NH_2-UiO-66, calculation method of conversion and TOF, the recyclability of the catalyst, GC analysis of the evolved gas from aqueous FA solution. See DOI: 10.1039/b000000x/

1 K. Tedsree, T. Li, S. Jones, C. A. Chan, K. M. K. Yu, P. A. J. Bagot, E. A. M. GeorgeD.W.Smith and S. C. E. Tsang, *Nat. Nanotechnol.*, 2011, **6**, 302-307.
2 J. A. Turner, *Science*, 2004, **305**, 972-974.
3 L. Schlapbach and A. Züttel, *Nature*, 2001, **414**, 353-358.
4 Q. Y. Bi, X. L. Du, Y. M. Liu, Y. Cao, H. Y. He and K. N. Fan, *J. Am. Chem. Soc.*, 2012, **134**, 8926-8933.
5 H.-L. Jiang and Q. Xu, *Catalysis Today*, 2011, **170**, 56-63.
6 T. Umegaki, A. Seki, Q. Xu and Y. Kojima, *J. Alloys Compd.*, 2014, **588**, 615-621.
7 Q.-L. Zhu and Q. Xu, *Energy Environ. Sci.*, 2015, **8**, 478-512.
8 X. Zhou, Y. Huang, W. Xing, C. Liu, J. Liao and T. Lu, *Chem. Commun.* , 2008, 3540-3542.
9 Y. Huang, X. Zhou, M. Yin, C. Liu and W. Xing, *Chem. Mater.*, 2010, **22**, 5122-5128.
10 X. Zhou, Y. Huang, C. Liu, J. Liao, T. Lu and W. Xing, *ChemSusChem*, 2010, **3**, 1379-1382.
11 X. Gu, Z. H. Lu, H. L. Jiang, T. Akita and Q. Xu, *J. Am. Chem. Soc.*, 2011, **133**, 11822-11825.
12 D. A. Bulushev, L. Jia, S. Beloshapkin and J. R. Ross, *Chem. Commun.*, 2012, **48**, 4184-4186.
13 M. Grasemann and G. Laurenczy, *Energy Environ. Sci.*, 2012, **5**, 8171-8181.
14 M. Yadav, T. Akita, N. Tsumori and Q. Xu, *J. Mater. Chem.*, 2012, **22**, 12582-12586.
15 O. Metin, X. Sun and S. Sun, *Nanoscale*, 2013, **5**, 910-912.
16 K. Mori, M. Dojo and H. Yamashita, *ACS Catal.*, 2013, **3**, 1114-1119.
17 Z. L. Wang, J. M. Yan, Y. Ping, H. L. Wang, W. T. Zheng and Q. Jiang, *Angew. Chem. Int. Ed.*, 2013, **52**, 4406-4409.
18 E. A. Bielinski, P. O. Lagaditis, Y. Zhang, B. Q. Mercado, C. Wurtele, W. H. Bernskoetter, N. Hazari and S. Schneider, *J. Am. Chem. Soc.*, 2014, **136**, 10234-10237.
19 C. Hu, J. K. Pulleri, S.-W. Ting and K.-Y. Chan, *Int. J. Hydrogen Energy*, 2014, **39**, 381-390.
20 K. Jiang, K. Xu, S. Zou and W. B. Cai, *J. Am. Chem. Soc.*, 2014, **136**, 4861-4864.
21 Y.-l. Qin, J.-w. Wang, Y.-m. Wu and L.-m. Wang, *RSC Adv.*, 2014, **4**, 30068-30073.
22 X. Wang, G.-W. Qi, C.-H. Tan, Y.-P. Li, J. Guo, X.-J. Pang and S.-Y. Zhang, *Int. J. Hydrogen Energy*, 2014, **39**, 837-843.
23 Z. L. Wang, H. L. Wang, J. M. Yan, Y. Ping, S. I. O, S. J. Li and Q. Jiang, *Chem. Commun.*, 2014, **50**, 2732-2734.
24 F. de Bruijn, *Green Chem.*, 2005, **7**, 132-150.
25 C. Fellay, P. J. Dyson and G. Laurenczy, *Angew. Chem. Int. Ed.*, 2008, **47**, 3966-3968.
26 B. Loges, A. Boddien, H. Junge and M. Beller, *Angew. Chem. Int. Ed.*, 2008, **47**, 3962-3965.
27 A. Boddien, B. Loges, H. Junge, F. Gärtner, J. R. Noyes and M. Beller, *Adv. Synth. Catal.*, 2009, **351**, 2517-2520.
28 Y. Chen, Q. L. Zhu, N. Tsumori and Q. Xu, *J. Am. Chem. Soc.*, 2015, **137**, 106-109.
29 S. Zhang, O. Metin, D. Su and S. Sun, *Angew. Chem. Int. Ed.*, 2013, **52**, 3681-3684.
30 A. K. Singh and Q. Xu, *ChemCatChem*, 2013, **5**, 652-676.
31 Z. L. Wang, J. M. Yan, Y. F. Zhang, Y. Ping, H. L. Wang and Q. Jiang, *Nanoscale*, 2014, **6**, 3073-3077.
32 S. Jones, J. Qu, K. Tedsree, X. Q. Gong and S. C. Tsang, *Angew. Chem. Int. Ed.*, 2012, **51**, 11275-11278.
33 J.-M. Yan, Z.-L. Wang, L. Gu, S.-J. Li, H.-L. Wang, W.-T. Zheng and Q. Jiang, *Adv. Energy Mater.*, 2015, DOI: 10.1002/aenm.201500107.
34 Q.-L. Zhu, N. Tsumori and Q. Xu, *Chem. Sci.*, 2014, **5**, 195-199.
35 Q. L. Zhu and Q. Xu, *Chem Soc Rev*, 2014, **43**, 5468-5512.
36 H. Dai, N. Cao, L. Yang, J. Su, W. Luo and G. Cheng, *J. Mater. Chem. A*, 2014, **2**, 11060-11064.
37 H. Dai, B. Xia, L. Wen, C. Du, J. Su, W. Luo and G. Cheng, *Appl. Catal. B*, 2015, **165**, 57-62.
38 J. Long, S. Wang, Z. Ding, Y. Zhou, L. Huang and X. Wang, *Chem. Commun.*, 2012, **48**, 11656-11658.

39 L. Shen, S. Liang, W. Wu, R. Liang and L. Wu, *Dalton Trans*, 2013, **42**, 13649-13657.
40 L. Shen, S. Liang, W. Wu, R. Liang and L. Wu, *J. Mater. Chem. A*, 2013, **1**, 11473-11482.
41 L. Shen, W. Wu, R. Liang, R. Lin and L. Wu, *Nanoscale*, 2013, **5**, 9374-9382.
42 D. Sun, Y. Fu, W. Liu, L. Ye, D. Wang, L. Yang, X. Fu and Z. Li, *Chem. Eur. J.*, 2013, **19**, 14279-14285.
43 J. Ethiraj, E. Albanese, B. Civalleri, J. G. Vitillo, F. Bonino, S. Chavan, G. C. Shearer, K. P. Lillerud and S. Bordiga, *ChemSusChem*, 2014, **7**, 3382-3388.
44 L. Shen, L. Huang, S. Liang, R. Liang, N. Qin and L. Wu, *RSC Adv.*, 2014, **4**, 2546-2549.
45 L. Shen, W. Wu, R. Liang, R. Lin and L. Wu, *Nanoscale*, 2013, **5**, 9374-9382.

Ag-Pd alloy supported on amine-functionalized UiO-66 as an efficient synergetic catalyst for dehydrogenation of formic acid at room temperature

Shu-Tao Gao, Weihua Liu, Cheng Feng*, Ning-Zhao Shang, Chun Wang*

College of Science, Agricultural University of Hebei, Baoding 071001, China

Highly dispersed Ag-Pd alloy deposited on amine-functionalized UiO-66(NH_2-UiO-66) have been successfully prepared with a pre coordination method. The as-synthesized AgPd@NH_2-UiO-66 catalyst exhibited 100% H_2 selectivity and high catalytic activity (TOF = 103 h^{-1}) toward the dehydrogenation of formic acid at room temperature without any additives.